

Upcycling of Dyed Polyester Fabrics into Copper-1,4-Benzenedicarboxylate (CuBDC) Metal–Organic Frameworks

Yelin Ko, Tyler J. Azbell, Phillip Milner, and Juan Hinestrosa*



Cite This: <https://doi.org/10.1021/acs.iecr.3c00226>



Read Online

ACCESS |

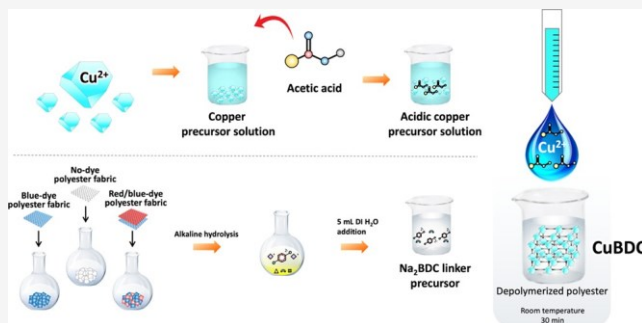
Metrics & More

Article Recommendations

Supporting Information

ABSTRACT: We report on a pathway to synthesize metal–organic frameworks (MOFs) using discarded textiles as a raw material. Discarded objects made of poly(ethylene terephthalate) (PET) could be an inexpensive and globally available source for 1,4-benzenedicarboxylic acid (H₂BDC), also known as terephthalic acid, a building block of carboxylate-based MOFs. Previous studies on using discarded PET to synthesize MOFs have mainly focused on PET bottles. In contrast, we demonstrate the use of dyed polyester fabrics as a raw material. Specifically, we report on a synthesis path for copper-1,4-benzenedicarboxylate (CuBDC) utilizing disodium terephthalate (Na₂BDC) as a linker and on how we obtained the linker from depolymerized polyester fabrics.

To facilitate coordination between the copper ions and Na₂BDC and create a localized acidic environment that favors the synthesis of CuBDC MOFs rather than metal oxide byproducts, we added acetic acid to the copper precursor solution. The drop-sized pH-controlled domain enabled the formation of CuBDC MOF crystals at room temperature and at a fraction of time shorter than traditional solvothermal methods. We confirmed the resulting MOF structures using powder X-ray diffraction (PXRD), scanning electron microscopy (SEM), thermogravimetric analysis (TGA), and Fourier transform infrared (FTIR) spectroscopy, and our results were in quantitative agreement with previous reports. Furthermore, we used different copper salts as metal sources and different color-dyed polyester fabrics as linker sources, demonstrating the versatility of the proposed synthesis path. These results may open an avenue for using discarded textiles as a raw material and offer a more circular approach for managing textile waste.



INTRODUCTION

Textiles industries generate over 5% of the total global solid waste.¹ A report by U.S. Environmental Protection Agency in 2015 estimated that the average amount of discarded textile waste per person in the United States is approximately 32 kg per year. More than 85% of textile waste ends up in landfills, raising serious environmental concerns and highlighting the need for effective and sustainable strategies to handle it.² Polyester fibers account for 50% of the fiber market. Since the 1990s, the consumption of polyester fibers has grown at a rate of nearly 7% per year.³ Several chemical recycling pathways available for polyester include methanolysis,⁴ glycolysis,⁵ aminolysis,⁶ and hydrolysis.⁷ Hydrolysis decomposes polyester into 1,4-benzenedicarboxylic acid (H₂BDC) and ethylene glycol. H₂BDC is a main building block for the preparation of high-value compounds.^{8,9}

One attractive upcycling target for H₂BDC are carboxylate-based metal–organic frameworks (MOFs). MOFs have a wide range of applications including catalysis,¹⁰ gas separation,¹¹ oil/¹² water separation,¹² gas storage,¹³ sensing,¹⁴ and drug delivery.¹⁵ MOF synthesis often requires expensive raw materials, toxic organic solvents such as *N,N*-dimethylformamide (DMF), and harsh reaction conditions.¹⁶ H₂BDC obtained from depolymerizing poly(ethylene terephthalate) (PET) can be obtained at

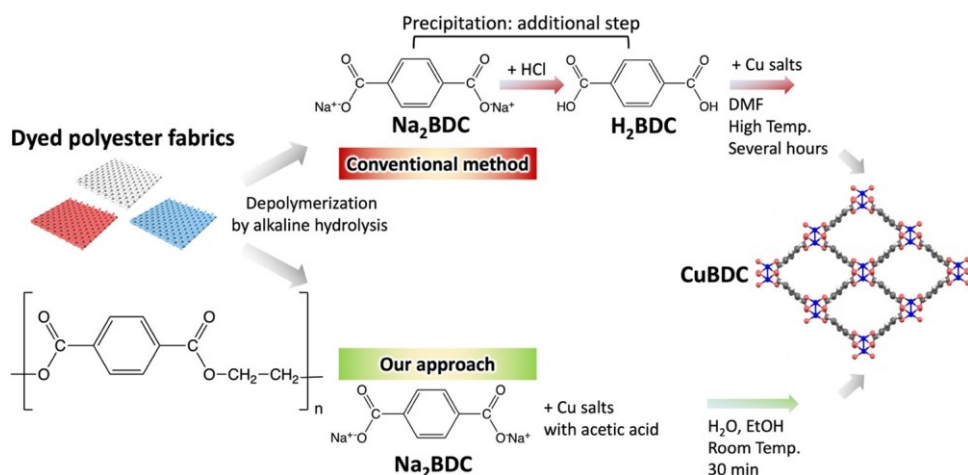
high purity levels^{7,17} and used as an organic linker in MOF assembly. Some researchers have demonstrated PET-to-MOF upcycling using PET bottles. For instance, Doan et al. synthesized copper-1,4-benzenedicarboxylate (CuBDC) utilizing H₂BDC recovered from PET bottles and used the resulting MOF to remove dyes from an aqueous solution.¹⁸ Dyosiba et al. and Dyosiba et al. demonstrated that various sources of PET waste, including PET bottles,¹⁹ food trays, colored bottles, and recycled PET beads,²⁰ could be used as a source for H₂BDC and in the synthesis of UiO-66 (UiO: Universitetet i Oslo). Lo et al. used PET bottles as a starting material for the synthesis of MIL-47 (MIL: Materials Institute Lavoisier), MIL-53(Cr, Al, Ga),⁵⁹ and MIL-101(Cr) frameworks using a one-pot strategy.²¹

However, previous attempts to employ H₂BDC obtained from PET as a linker for MOF synthesis have suffered from several limitations. For example, most methods require

Received: January 22, 2023

Revised: March 19, 2023

Accepted: March 22, 2023

Scheme 1. Methods to Synthesize CuBDC MOFs from Dyed Polyester Fabrics^a

^aTop: A conventional pathway requiring protonation to isolate H₂BDC. Bottom: Our proposed approach which directly utilizes Na₂BDC available after depolymerization of polyester fabrics.

Table 1. Initial pH and Final pH of Copper Precursor Solutions after Adding Acetic Acid

copper salts	initial pH	amount of acetic acid added (mL)	final pH
Cu(NO ₃) ₂ ·3H ₂ O	3.02 ± 0.02	0.015	1.97 ± 0.02 (pH 2.0 condition)
		0.115	1.53 ± 0.03 (pH 1.5 condition)
		0.300	1.23 ± 0.01 (pH 1.2 condition)
Cu(CH ₃ COO) ₂ ·H ₂ O	6.65 ± 0.03	0.015	6.03 ± 0.02 (pH 6.0 condition)
		0.115	5.04 ± 0.03 (pH 5.0 condition)
		0.300	4.51 ± 0.04 (pH 4.5 condition)
CuSO ₄ ·5H ₂ O	4.31 ± 0.04	0.015	3.19 ± 0.02 (pH 3.2 condition)
		0.115	2.67 ± 0.03 (pH 2.7 condition)
		0.300	2.49 ± 0.01 (pH 2.5 condition)

⁶⁴ deprotonation of H₂BDC, which necessitates the inclusion of at
⁶⁵ least one of the following steps: (1) isolation of H₂BDC,
⁶⁶ involving a series of subsequent steps such as precipitation,
⁶⁷ filtration, and drying; (2) use of a toxic organic solvent such as
⁶⁸ DMF to dissolve H₂BDC; or (3) use of solvothermal method
⁶⁹ requiring high reaction temperature.

⁷⁰ An approach that utilizes an already-deprotonated linker
⁷¹ (BDC²⁻) instead of the linker conjugated acid (H₂BDC), as a
⁷² MOF precursor, could potentially overcome these restrictions.
⁷³ However, although several reports have partially demonstrated
⁷⁴ the feasibility of this approach for the preparation of MOF
⁷⁵ structures,^{22,23} direct conversion of a BDC²⁻ salt obtained from
⁷⁶ depolymerized PET into a MOF has not yet been explored. We
⁷⁷ propose that as alkaline hydrolysis decomposes PET into
⁷⁸ Na₂BDC, using the deprotonated linker available after PET
⁷⁹ depolymerization would eliminate the need for additional
⁸⁰ protonation/precipitation steps (Scheme 1).

⁸¹ To prevent copper ions from coordinating with a hydroxide
⁸² ion and forming insoluble impurities such as Cu(OH)₂ or CuO
⁸³ under alkaline reaction conditions,²⁴ we added acetic acid
⁸⁴ (AcOH) to the copper precursor solutions. This approach

⁸⁵ allowed for the localized adjustment of the pH value of the
⁸⁶ copper precursor drops inside the alkaline depolymerization
⁸⁷ solution, creating localized conditions that favored MOF
⁸⁸ assembly. Our approach uses ethanol and water as solvents
⁸⁹ and requires a reaction time of 30 min at room temperature,
⁹⁰ which is significantly faster than previous reports in which toxic
⁹¹ solvents and higher reaction temperatures have been used.²⁵

We used no-dye polyester, blue-dye polyester, and a 50/50 mixture (by weight) of red- and blue-dye polyester fabrics as raw materials and characterized the purity of the H₂BDC obtained from each source. We also determined the optimal pH values for MOF formation using several copper salts such as Cu(NO₃)₂·3H₂O, Cu(CH₃COO)₂·H₂O, and CuSO₄·5H₂O. These experiments provided insights into the role of the copper precursor solution's pH on the properties of resulting MOF structures.

EXPERIMENTAL SECTION

Materials. Polyester fabrics without any dyes (100% polyester knit, lot 2926), with blue dye (100% polyester knit, disperse dye blue, lot 6554), and with red dye (100% polyester knit, disperse dye rust, lot 3044) were purchased from Testfabrics, Inc. Cu(NO₃)₂·3H₂O (Sigma-Aldrich, 99%), Cu(CH₃COO)₂·H₂O (Sigma-Aldrich, 99%), CuSO₄·5H₂O (Sigma-Aldrich, 98%), terephthalic acid (Sigma-Aldrich, 98%), hydrochloric acid (EMD Millipore, 36.5–38.0%), acetic acid (Macron Fine Chemicals, 99.7%), sodium hydroxide (Macron Fine Chemicals), and ethanol (Koptec, 100%) were used as received without further purification.

Depolymerization of Polyester Fabrics. Polyester fabrics weighing 0.2 g were placed into a round-bottom flask containing 7 mL of 0.7 M sodium hydroxide solution (6 mL of ethanol and 1 mL of deionized water, DI water). Each flask was heated in a silicone oil bath at 80 °C for 3 h under magnetic stirring. A water-cooled reflux condenser was placed on top of the reaction flask. In a separate experiment, to determine the maximum amount of recoverable H₂BDC, hydrochloric acid was added

120 into the depolymerization mixture until the pH of the mixture
121 reached 2.0. The resulting crystalline solid was filtered and dried
122 in an oven at 100 °C for 4 h.

123 **Room-Temperature Synthesis of CuBDC MOFs.** To
124 increase the solubility of the Na₂BDC linker, 5 mL of DI water
125 was added to the solution containing the depolymerized
126 polyester fabrics. Separately, a metal precursor solution was
127 prepared by dissolving each of the copper salts (Cu(NO₃)₂·
128 3H₂O, Cu(CH₃COO)₂·H₂O, and CuSO₄·5H₂O) in 12 mL of a
129 solvent. Ethanol was used as the solvent for Cu(NO₃)₂·3H₂O
130 and Cu(CH₃COO)₂·H₂O, and DI water was used as the solvent
131 for CuSO₄·5H₂O. Acetic acid was added to each copper salt
132 solution in the following amounts: 0.015, 0.115, and 0.300 mL.
133 The values for the initial pH of the copper precursor solutions
134 and their final pH after the addition of acetic acid are shown in
135 **Table 1.**

Table 2. % Yield of H₂BDC Recovered from Depolymerized Polyester Fabrics

	polyester fabric (g)	H ₂ BDC recovered (g)	H ₂ BDC yield (%)
no-dye polyester	0.2	0.1689 ± 0.001	99.35
blue-dye polyester	0.2	0.1610 ± 0.001	94.73
50/50 mixture of red and blue-dye polyester	0.2	0.1600 ± 0.001	94.12

136 The acidic copper precursor solution was added dropwise to
137 the depolymerization solution under magnetic stirring at room
138 temperature leading to the immediate precipitation of a blue
139 solid. After adding the total amount of the copper solution for
140 each experiment into the depolymerization mixture, the
141 contents were stirred for an additional 30 min before collecting
142 the solids via centrifugation.

143 The solids were transferred to a tube and washed with 5 mL of
144 DI water using an ultrasonic bath sonicator. After adding 9 mL of
145 ethanol, the tube was placed in a 900 rpm vortexer. The resulting
146 solids were redispersed in ethanol and dried in an oven at 75 °C
147 overnight prior to their characterization.

148 **Characterization of the Resulting H₂BDC Linker and**
149 **CuBDC MOF Structures.** Powder X-ray diffraction (PXRD)
150 patterns of CuBDC MOFs were collected using a Bruker D8
151 Advance ECO powder diffractometer equipped with Cu K α
152 radiation (40 kV, 25 mA, wavelength $\lambda = 1.5606 \text{ \AA}$) at a scan
153 speed of 0.03°·s⁻¹. Nuclear magnetic resonance (NMR) spectra

154 of H₂BDC were obtained at 500.03 MHz (¹H) and at 125.75 MHz
155 (¹³C) on a Bruker AVIII spectrometer equipped with a
156 broadband Prodigy cryoprobe. The spectra were processed
157 using MNova (v. 14.3, Mestrelab Research S. L.) software.
158 Thermogravimetric analysis (TGA) of H₂BDC and CuBDC
159 MOFs was carried out in a TGA analyzer (Q500, TA
160 Instruments) by heating the samples from 25 to 600 °C in a
161 N₂ atmosphere at a heating rate of 10 °C·min⁻¹. Differential
162 scanning calorimetry (DSC) of H₂BDC was performed using a
163 TA Instruments Q2000 system heated from 40 to 400 °C at a
164 rate of 5 °C·min⁻¹. Fourier transform infrared (FTIR) spectra of
165 H₂BDC and CuBDC MOFs were obtained by a PerkinElmer
166 FTIR spectrophotometer on a range of 4000–600 cm⁻¹.
167 Scanning electron microscopy (SEM) images of CuBDC
168 MOFs coated with a thin carbon layer were collected at a
169 voltage of 2.0 kV using a Zeiss Gemini 500 Scanning Electron
170 Microscope. Surface area measurements of CuBDC MOFs were
171 obtained on a Micromeritics ASAP 2460 gas sorption analyzer
172 using ultrapure N₂ (99.999%) and a liquid N₂ bath. The
173 Brunauer–Emmett–Teller (BET) surface areas of CuBDC
174 MOFs were determined by a linear least squares regression
175 analysis using the linearized form of the BET equation. The
176 Barrett–Joyner–Halenda model (BJH) was used to determine
177 the average pore diameter and pore size distribution.
178

RESULTS AND DISCUSSION

179 **Purity of Terephthalic Acid Obtained after Polyester**
180 **Depolymerization.** The obtained H₂BDC powders were
181 white, purple-gray, and pink when no-dye polyester, blue-dye
182 polyester, and the 50/50 mixture of red and blue-dye polyester
183 fabrics were used as precursors, respectively (Figure S1). The
184 yield for obtaining H₂BDC was calculated using eq 1, where
185 $m_{\text{H}_2\text{BDC}}$ is the mass of the H₂BDC after the depolymerization
186

187 reaction and m_{PET} is the mass of polyester fabrics used (Table
188 2). The coefficient of 0.85 represents the theoretical ratio of the
189 molecular weight of BDC units ($C_8H_4O_4$, 164.11 g·mol⁻¹) to
190 that of ethylene terephthalate repeating units ($C_{10}H_8O_4$, 192.17
191 g·mol⁻¹).⁹

$$\text{H}_2\text{BDC yield (\%)} = \frac{m_{\text{H}_2\text{BDC}}}{m_{\text{PET}} \times 0.85} \times 100 \quad (1)$$

192 The ¹H and ¹³C NMR spectra of the H₂BDC obtained from
193 the depolymerized polyester fabrics were recorded and
194 compared to the spectra of commercial H₂BDC. The NMR
195

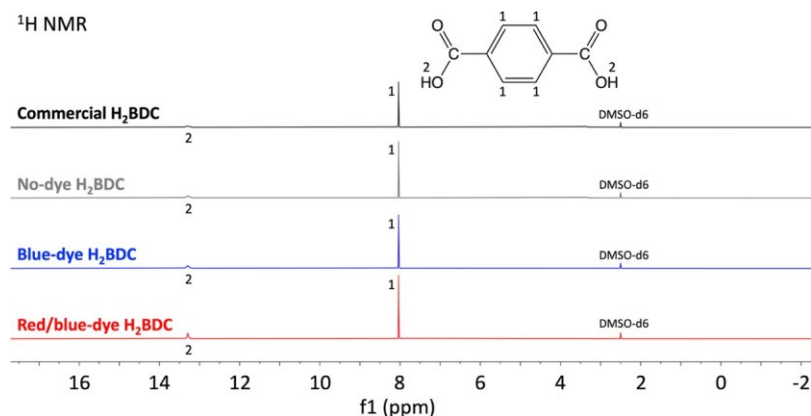


Figure 1. ¹H NMR spectra of commercial H₂BDC, H₂BDC recovered from no-dye polyester, H₂BDC recovered from blue-dye polyester, H₂BDC recovered from the 50/50 mixture of red and blue-dye polyester fabrics.

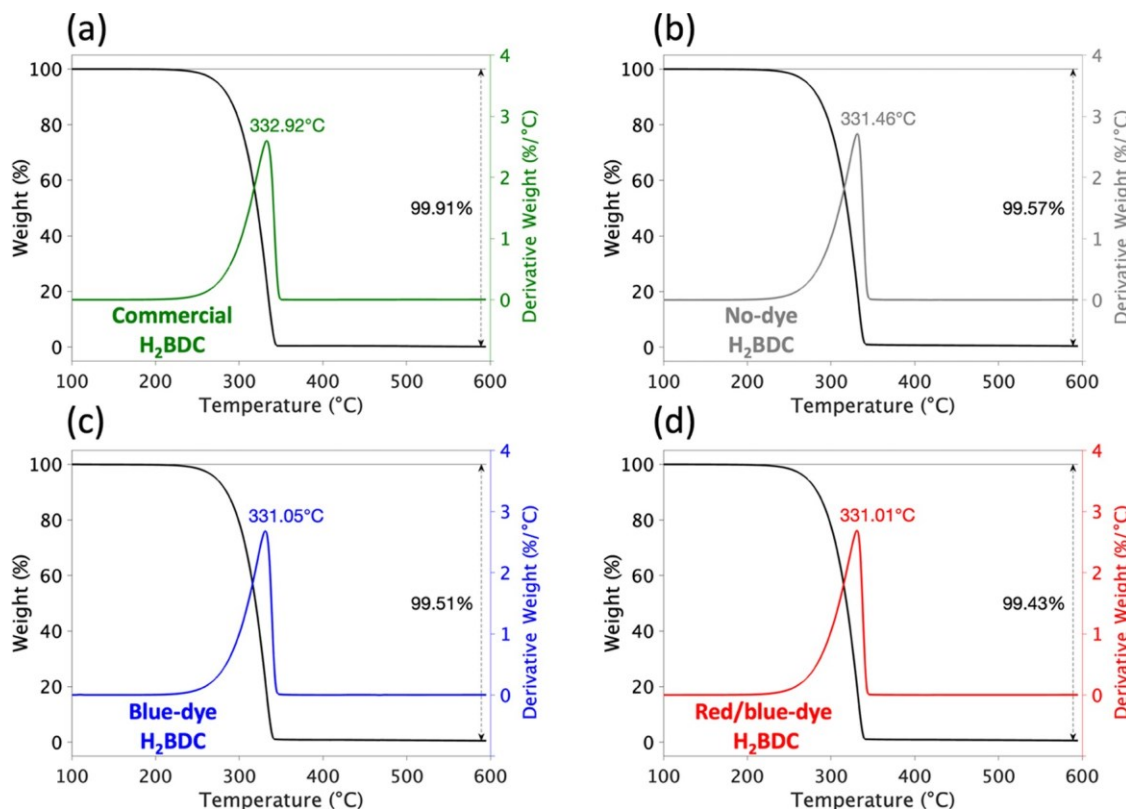


Figure 2. TGA curves of H₂BDC: (a) commercial H₂BDC, (b) H₂BDC from no-dye polyester, (c) H₂BDC from blue-dye polyester, and (d) H₂BDC from the 50/50 mixture of red and blue-dye polyester fabrics.

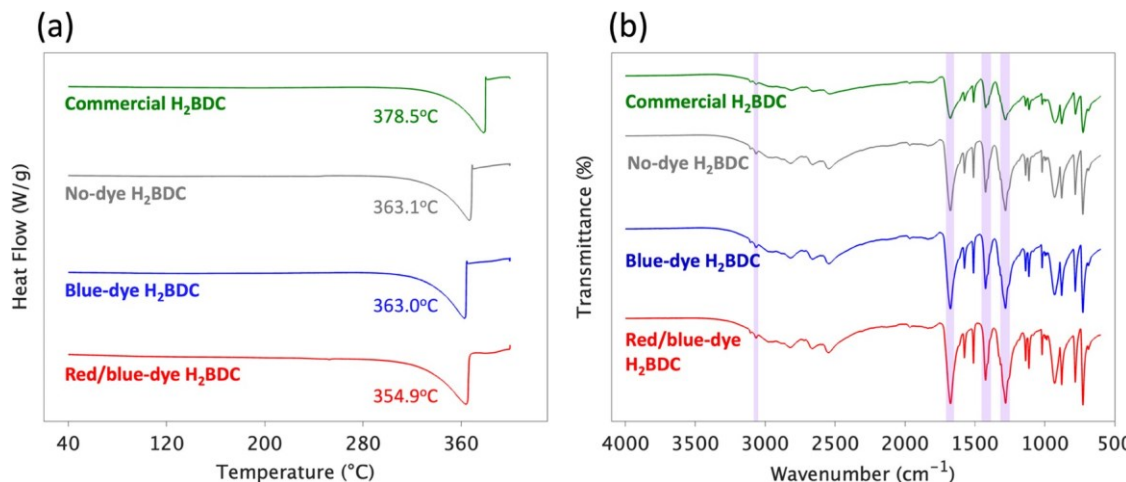


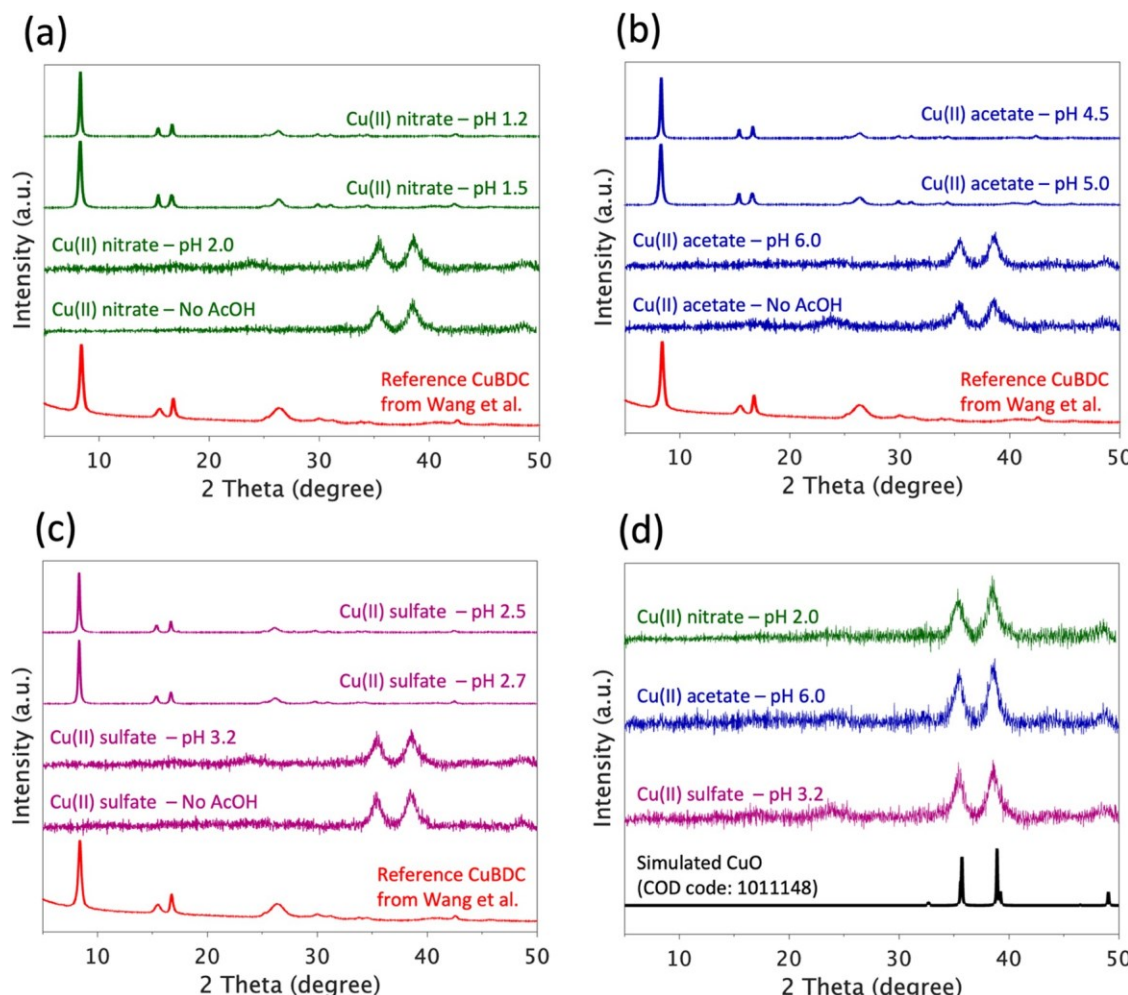
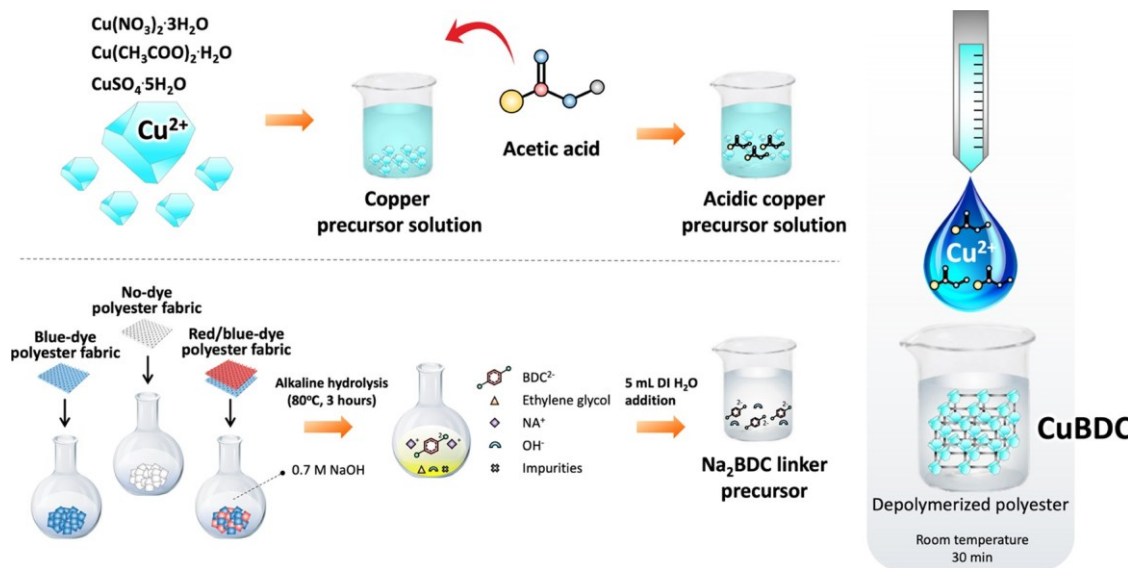
Figure 3. (a) DSC thermogram and (b) FTIR spectra of commercial H₂BDC and H₂BDC recovered from no-dye polyester, blue-dye polyester, and the 50/50 mixture of red and blue-dye polyester fabrics.

195 spectra for both ¹H and ¹³C were identical (Figures 1 and S2).
 196 The signals at 8.04 and 13.29 ppm in ¹H NMR (Figure 1)
 197 spectra correspond to the protons of the benzene ring and the
 198 carboxylic acid group.²⁷ Based on the ¹H NMR analysis, the
 199 purity of H₂BDC recovered from the no-dye polyester, blue-dye
 200 polyester, and the 50/50 mixture of red and blue-dye polyester
 201 fabrics was 99.6, 99.5, and 98.7%, respectively. These results
 202 indicate that the presence of dyes had a negligible effect on the
 203 chemical structure of the recovered H₂BDC.

204 TGA thermograms are presented in Figure 2. The H₂BDC
 205 recovered from the depolymerized no-dye polyester, blue-dye
 206 polyester, and the 50/50 mixture of red and blue-dye polyester

207 fabrics, as well as the commercially available H₂BDC, exhibited a
 208 similar single-step decomposition pattern with a large peak
 209 around 332 °C, which is in quantitative agreement with
 210 previously reported values for the sublimation of H₂BDC.²⁶
 211 Both the H₂BDC recovered from the polyester fabrics and the
 212 commercial H₂BDC completely decomposed when heated up to
 213 600 °C. Similarly, the DSC curves of the recovered H₂BDC
 214 obtained from the depolymerized polyester fabrics and the
 215 commercial H₂BDC showed the absence of any melting
 216 transition, as shown in Figure 3a.^{17,28} The intense endothermic
 217 peak of the H₂BDC obtained from the polyester depolymeriza-
 218 tion appeared at slightly lower temperatures compared to that of
 219

Scheme 2. Schematic Illustration of Our Approach to Synthesize CuBDC MOFs Using Polyester Fabrics

Figure 4. PXRD patterns of samples obtained using different copper precursor solutions at different pH values: (a) $\text{Cu}(\text{NO}_3)_2 \cdot 3\text{H}_2\text{O}$, (b) $\text{Cu}(\text{CH}_3\text{COO})_2 \cdot \text{H}_2\text{O}$, (c) $\text{CuSO}_4 \cdot 5\text{H}_2\text{O}$, and (d) comparison between simulated CuO and byproduct compounds obtained at higher pH values.

219 the commercial H_2BDC (Figure 3a), but the difference falls
 220 within reported ranges.^{29,30} The thermogravimetric and DSC
 221 analyses are in agreement with the NMR data and confirm the

high purity of the recovered H_2BDC from the colored polyester
 222 fabrics.
 223

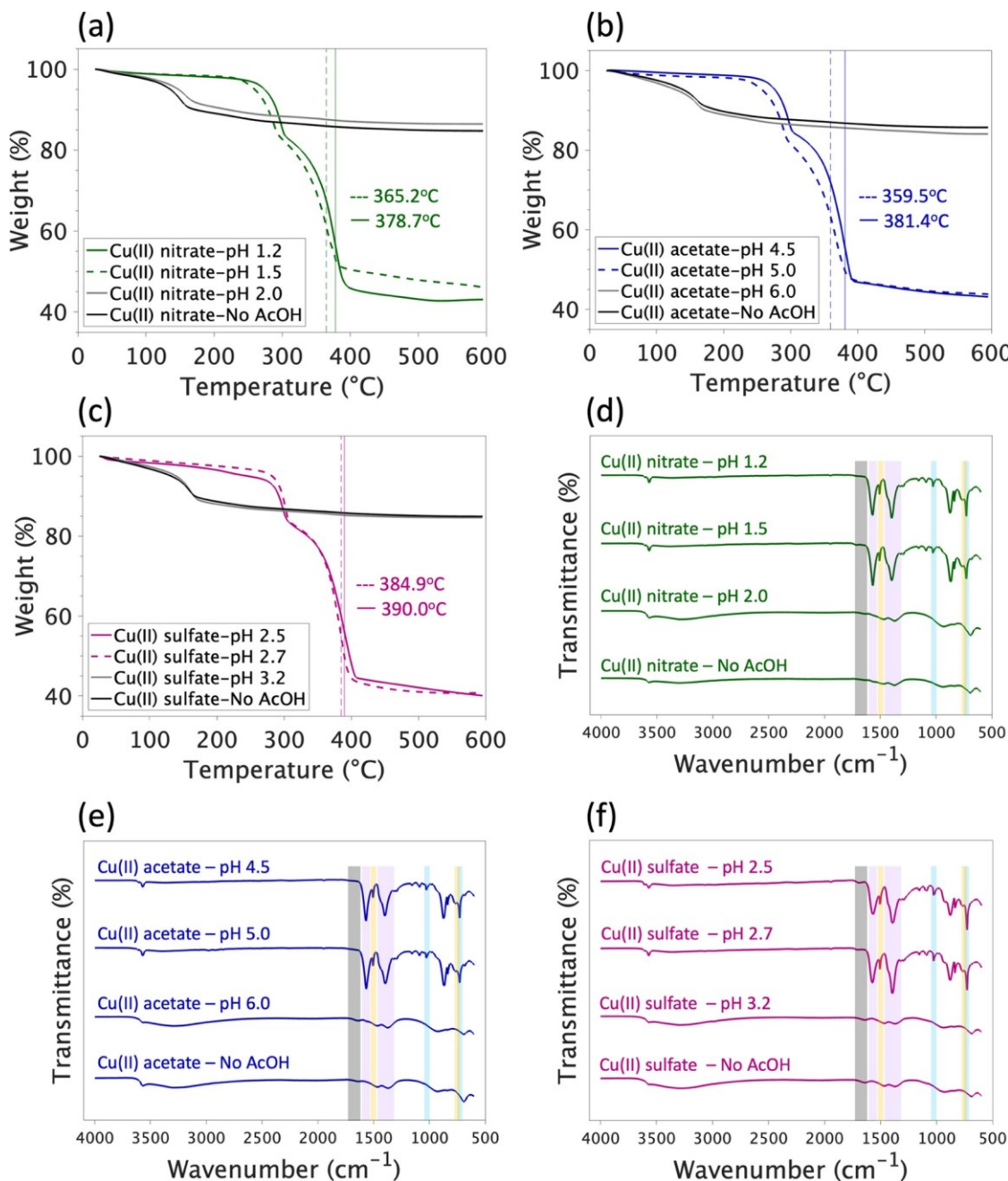


Figure 5. TGA curves (a-c) and FTIR spectra (d-f) of samples synthesized using Na₂BDC obtained from no-dye polyester fabrics and different copper salts: (a, d) Cu(NO₃)₂·3H₂O, (b, e) Cu(CH₃COO)₂·H₂O, and (c, f) CuSO₄·5H₂O.

The FTIR characteristic peaks of the H₂BDC obtained from the depolymerized polyester fabrics also matched those of the commercial H₂BDC and those reported in the literature,³¹ as shown in Figure 3b. The peak at 3064 cm⁻¹ is attributed to the C–H stretching of the benzene ring, while the peak at 1685 cm⁻¹ indicates the presence of C=O stretching. The peaks at 1424 and 1285 cm⁻¹ correspond to OH in-plane deformation and ether C–O stretching.

Synthesis of CuBDC Using Polyester Fabrics as a Linker Source. The approach we used to synthesize CuBDC MOFs from depolymerized polyester fabrics is described in Scheme 2. Different copper salts were considered as metal precursors, and to prevent copper ions from forming impurities,

acetic acid was added to the copper precursor solution before it was added dropwise to the alkaline depolymerization solution.

Experiments with No-Dye Polyester Fabrics. Before conducting synthesis experiments with dyed polyester fabrics, baseline experiments were performed using no-dye polyester fabrics to investigate the effect of the copper precursor solutions' pH on the formation of CuBDC MOF structures. The PXRD patterns shown in Figure 4 indicate that the precipitates formed using copper solutions with no acetic acid or with lower amounts of acetic acid (pH 2.0 for Cu(NO₃)₂·3H₂O, pH 6.0 for Cu(CH₃COO)₂·H₂O, and pH 3.2 for CuSO₄·5H₂O solution) contained Cu-based byproducts such as CuO (Code of Crystallography Open Database, COD: 1011148) (Figure 4d). These impurities can be attributed to the hindered

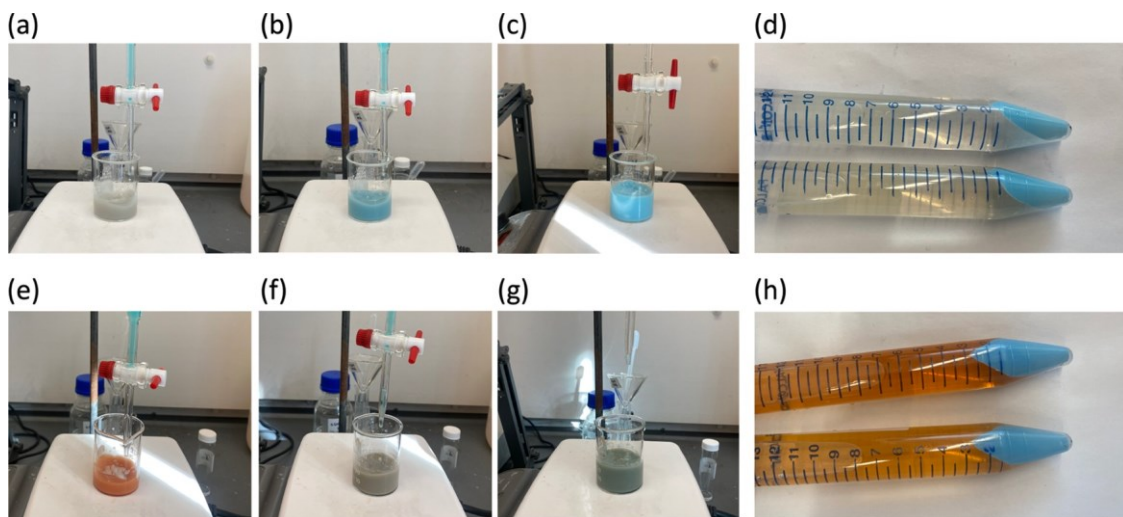


Figure 6. Digital photos of the room-temperature CuBDC MOFs synthesis using Na_2BDC from depolymerized blue-dye polyester (top) and a 50/50 mixture of red and blue-dye polyester fabrics (bottom): (a, e) before adding the Cu/AcOH solution at pH 4.5, (b, f) while adding the Cu/AcOH solution, (c, g) after completion of the reaction, (d, h) blue solids and colored supernatant obtained after centrifugation.

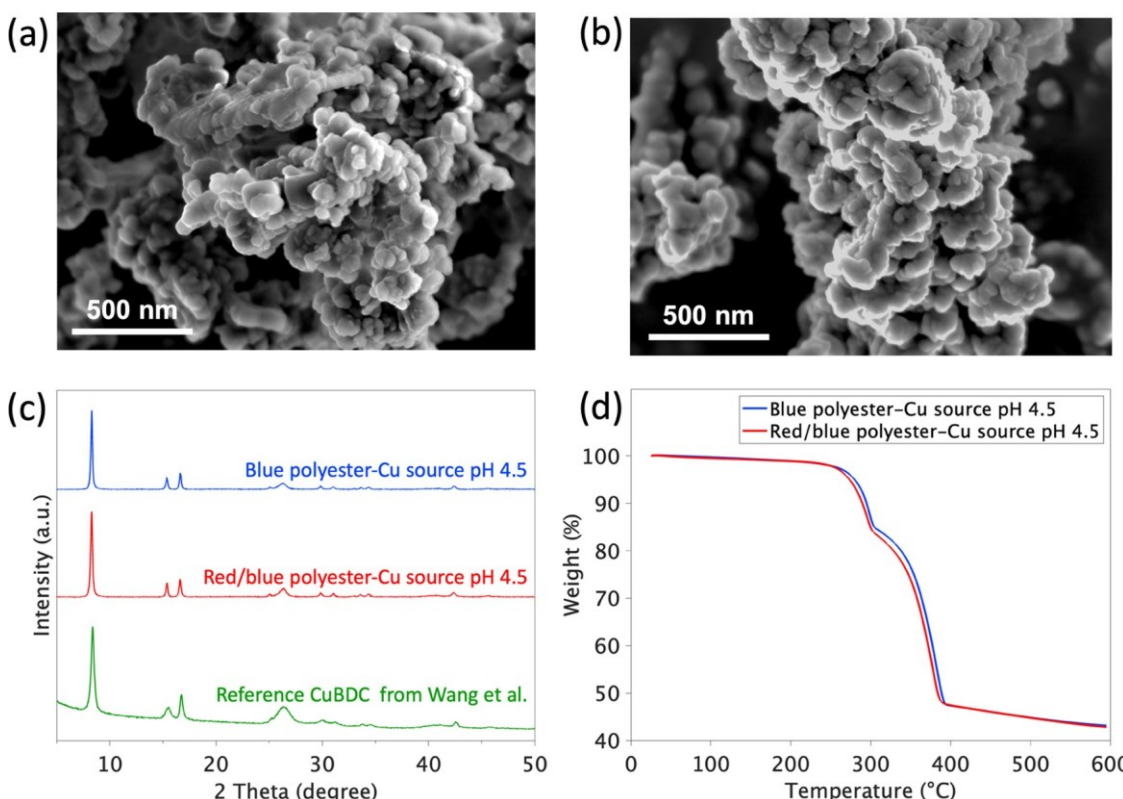


Figure 7. Characterization of CuBDC MOFs synthesized using Na_2BDC from depolymerized blue-dye polyester and the 50/50 mixture of red and blue-dye polyester fabrics and the copper acetate solutions at pH 4.5: (a) SEM image of CuBDC MOFs obtained from blue-dye polyester fabrics, (b) SEM image of CuBDC MOFs obtained from the 50/50 mixture of red and blue-dye polyester fabrics, (c) PXRD patterns, and (d) TGA curves.

formation of dimeric copper centers in the copper paddlewheel clusters—the most critical step in CuBDC MOF crystallization—leading to Cu-based byproducts known to occur under basic conditions.²⁴ In contrast, all structures formed at lower pH values produced phase-pure CuBDC MOFs (Figure 4a–c), and their PXRD patterns were in quantitative agreement with those reported by Wang et al.³² and others.^{33–36}

The thermal stability of the samples synthesized using Na_2BDC obtained from no-dye polyester fabrics and three

different copper salts was evaluated using TGA, as shown in Figure 5a–c. Similar to their corresponding PXRD patterns, samples synthesized using larger amounts of acetic acid (below pH 1.5 for $\text{Cu}(\text{NO}_3)_2 \cdot 3\text{H}_2\text{O}$ solution, pH 5.0 for $\text{Cu}(\text{CH}_3\text{COO})_2 \cdot \text{H}_2\text{O}$ solution, pH 2.7 for $\text{CuSO}_4 \cdot 5\text{H}_2\text{O}$ solution) exhibited a two-stage weight loss, which is common for CuBDC MOFs.^{18,22} The first stage of weight loss (16–17%) is likely due to the removal of the water and ethanol solvent. The second stage of weight loss appeared between approximately 300 and 600

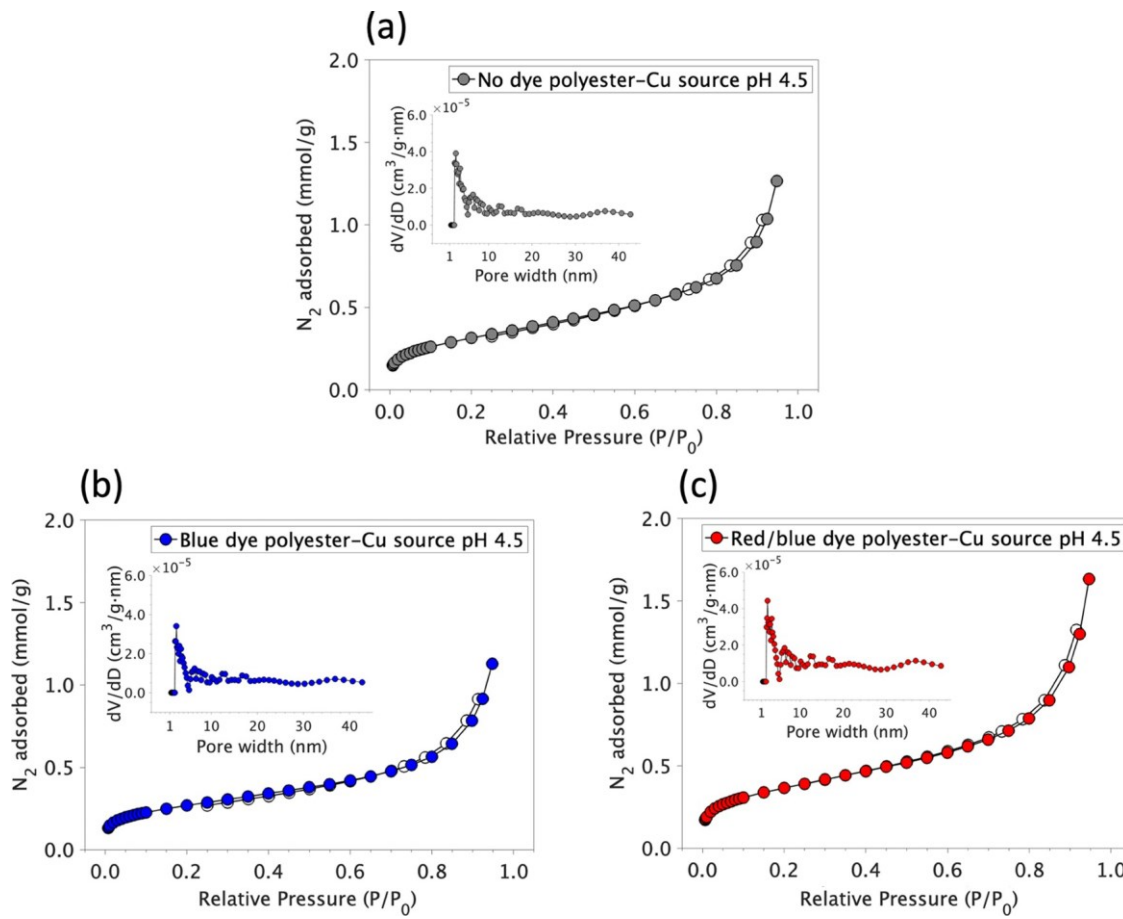


Figure 8. Nitrogen sorption (closed circles) and desorption (open circles) isotherms for CuBDC MOFs synthesized using Na_2BDC from depolymerized polyester fabrics and copper acetate solutions at pH 4.5. The inset corresponds to pore diameter distributions: (a) no-dye polyester, (b) blue-dye polyester, and (c) the 50/50 mixture of blue and red-dye polyester fabrics.

400 °C, accounting for 34–39% of the initial weight. This loss is attributable to the decomposition of the organic linker.³⁸ The residue after 400 °C corresponds to CuO, which is thermally stable up to 600 °C. According to the literature, CuBDC MOF structures at high temperatures collapse into CuO.³⁹

The chemical composition of the samples synthesized using Na_2BDC recovered from no-dye polyester fabrics and three different copper salts was also evaluated using FTIR, as shown in Figure 5d–f. The FTIR spectra are in quantitative agreement with previously reported spectra for CuBDC MOFs.^{25,37} The characteristic peaks at 1566 and 1394 cm^{-1} correspond to COO^- antisymmetric and symmetric stretching vibrations. The peaks at 1500 and 775 cm^{-1} match the vibrations specific to the phenyl ring, while the C–H vibrations in the aromatic ring are evident at 1025 and 738 cm^{-1} .^{25,37} The carbonyl peaks related to the protonated carboxyl group are assigned to 1710–1760 cm^{-1} .

After demonstrating the synthesis of pure CuBDC MOFs using depolymerized undyed polyester fabrics, we turned our attention to exploring the potential scale-up of the synthesis reaction using dyed polyester fabrics. To this end, we chose to use $\text{Cu}(\text{CH}_3\text{COO})_2 \cdot \text{H}_2\text{O}$ as the copper source. Water can react with metal oxide clusters, causing ligand displacement⁴⁰ and slowly hydrolyzing the symmetrical bidentate carboxylate ligands bonded to the copper cations.⁴¹ Therefore, we did not use $\text{CuSO}_4 \cdot 5\text{H}_2\text{O}$, which is soluble in water but not in ethanol. We also decided against using $\text{Cu}(\text{NO}_3)_2 \cdot 3\text{H}_2\text{O}$ due to its higher

cost and the need for extra safety precautions when it is used in large amounts.⁴²

Experiments with Dyed Polyester Fabrics. We used polyester fabrics containing blue and red dyes to assess the robustness of the crystallization during the assembly of MOF structures using a pH 4.5 copper acetate solution. As shown in Figure 6a–c, blue-dye polyester fabrics depolymerized into a gray-purple solution that eventually turned blue after the addition of the acidic copper acetate solution. The depolymerized solution obtained from the 50/50 mixture of red and blue-dye polyester fabrics changed from orange to cloudy khaki after adding the copper acetate solution, as shown in Figure 6e–g. After centrifugation, we observed that a dye-containing liquid remained in the supernatant while the blue solids precipitated (Figure 6d,h).

The isolated blue solids were characterized by SEM, PXRD, TGA, and FTIR spectra, as shown in Figures 7 and S3. The morphology of the CuBDC MOFs samples synthesized from blue-dye polyester (Figure 7a) and the 50/50 mixture of red and blue-dye polyester fabrics (Figure 7b) appeared similar in the SEM images and exhibited a granular structure that qualitatively agrees with those of the reported literature.^{14,25} All tested samples exhibited the same CuBDC crystal structure as reported by Wang et al.³² and others (Figure 7c).^{33–36} The TGA thermograms indicated that the CuBDC MOF structures synthesized with dyed polyester fabrics showed a two-step weight loss pattern, similar to those of the CuBDC MOF

322 samples synthesized with no-dye polyester fabrics (Figure 7d).
 323 The rapid weight loss appeared at 382.1 and at 377.2 °C for the
 324 CuBDC MOF samples prepared with blue-dye polyester and
 325 with the 50/50 mixture of red and blue-dye polyester fabrics,
 326 respectively. These values are comparable to those obtained
 327 using no-dye polyester fabrics. (Figure 5b). The FTIR spectra of
 328 both samples confirmed the presence of the characteristic peaks
 329 of CuBDC MOFs (Figure S3), which agree with those observed
 330 in the CuBDC MOFs structures obtained using no-dye
 331 polyester fabrics (Figure 5e) and with those reported in the
 332 literature.^{25,37}

333 Figure 8 shows nitrogen isotherms measured at 77 K to study
 334 the porosity of the CuBDC MOF samples prepared using no-
 335 dye and dyed polyester fabrics and a pH 4.5 copper acetate
 336 solution. The average pore diameters determined by the BJH
 337 method and total pore volumes are presented in Table 3. All

Table 3. Porous Properties of the As-Synthesized CuBDC MOFs Prepared Using Na₂BDC from No-Dye and Dyed Polyester Fabrics²

CuBDC MOFs	BET surface area (m ² ·g ⁻¹)	average pore diameter (nm)	total pore volume (cm ³ ·g ⁻¹)
no-dye/Cu source at pH 4.5	25 ± 0.21	7.06	0.044
blue-dye/Cu source at pH 4.5	21 ± 0.12	8.87	0.039
red/blue-dye/Cu source at pH 4.5	29 ± 0.17	8.90	0.057
CuBDC synthesized at RT by Li et al. ²²	49.6		
CuBDC synthesized at RT by Zhang et al. ²⁵	46.78		0.223
CuBDC synthesized at RT by Wang et al. ³²	87	1.4	
CuBDC synthesized at RT by Chen et al. ³³	33.27		

43,44
 38 samples tested exhibited a type II isotherm (Figure 8a-c),
 39 which is in agreement with previously reported data for CuBDC
 40 MOFs.²² The BET surface area values are also comparable with
 41 previously reported data for CuBDC MOFs synthesized using
 42 Na₂BDC at room temperature (Table 3).^{22,25,32,33} The N₂
 43 isotherm (Figure 8a-c) and porous properties (Table 3) of
 44 the CuBDC MOF samples synthesized using Na₂BDC from
 45 blue-dye polyester and the 50/50 mixture of red and blue-dye
 46 polyester fabrics were similar to those of CuBDC MOFs made
 47 using no-dye polyester fabrics. These findings further demon-
 48 strate the suitability of this pathway to synthesize CuBDC
 49 MOFs directly from a depolymerization mixture without the
 50 need for isolating H₂BDC.

CONCLUSIONS

51 We demonstrated the direct upcycling of dyed polyester fabrics
 52 into CuBDC MOFs. The reported approach directly utilizes
 53 Na₂BDC from a depolymerized solution without the need to
 54 precipitate and purify the H₂BDC linker. This approach avoids
 55 the use of toxic solvents and high reaction temperatures for
 56 crystallization and does not require additional steps for linker
 57 isolation, hence making it amenable to scale-up. We also
 58 determined that the reported approach allows for the use of
 59 different copper salts (Cu(NO₃)₂·3H₂O, Cu(CH₃COO)₂·H₂O,
 60 and CuSO₄·5H₂O), as well as dye-colored polyester fabrics,
 61 without affecting the structure of the resulting CuBDC MOFs.

These findings suggest that discarded textiles could be used as raw materials for MOF synthesis and highlight the selective crystallization properties of metal-organic frameworks. These results also demonstrate that MOF assembly provides an effective means to reject dye molecules and other impurities, enabling simplified separation of terephthalate from polyester fabric digestion mixtures.

As CuBDC MOF structures have already shown antibacterial and other functional properties, MOFs synthesized from discarded textiles could be incorporated as functional finishes for other substrates, potentially enabling a more circular approach for the textile industry.

ASSOCIATED CONTENT

Supporting Information

The Supporting Information is available free of charge at <https://pubs.acs.org/doi/10.1021/acs.iecr.3c00226>.

Digital photos and ¹³C NMR spectra of commercial H₂BDC, H₂BDC from no-dye polyester, blue-dye polyester, and the 50/50 mixture of red and blue-dye polyester fabrics; FTIR spectra of CuBDC MOFs synthesized using Na₂BDC from blue-dye polyester and the 50/50 mixture of red and blue-dye polyester fabrics and copper acetate solutions at pH 4.5 (PDF)

AUTHOR INFORMATION

Corresponding Author

Juan Hinestroza – Department of Human Centered Design, Cornell University, Ithaca, New York 14850, United States; orcid.org/0000-0002-8534-1407; Email: jh433@cornell.edu

Authors

Yelin Ko – Department of Human Centered Design, Cornell University, Ithaca, New York 14850, United States

Tyler J. Azbell – Department of Chemistry and Chemical Biology, Cornell University, Ithaca, New York 14850, United States

Phillip Milner – Department of Chemistry and Chemical Biology, Cornell University, Ithaca, New York 14850, United States; orcid.org/0000-0002-2618-013X

Complete contact information is available at:

<https://pubs.acs.org/10.1021/acs.iecr.3c00226>

Author Contributions

Y.K. performed most experiments and wrote the initial drafts. T.J.A. performed BET experiments and analysis of the data. P.M. provided guidance on the experimental setup and MOF synthesis strategies, as well as edited and reviewed the manuscript. J.H. performed initial planning of the experiments and analysis of the experimental data, as well as reviewed and edited the manuscript. The manuscript could not have been written without the contributions of all authors. All authors have given approval to the final version of the manuscript.

Notes

The authors declare no competing financial interest.

ACKNOWLEDGMENTS

The authors are grateful to Dr. Wang's group for providing them with the PXRD raw data used in their publication allowing them to create a better comparison with our structures.

419 **ABBREVIATIONS**

420 AcOH	acetic acid
421 BET	Brunauer–Emmett–Teller
422 BJH	Barrett–Joyner–Halenda
423 COD	crystallography open database
424 CuBDC	copper-1,4-benzenedicarboxylate
425 DI water	deionized water
426 DMF	<i>N,N</i> -dimethylformamide
427 DSC	differential scanning calorimetry
428 FTIR	Fourier transform infrared spectroscopy
429 H ₂ BDC	1,4-benzenedicarboxylic acid
430 MOFs	metal–organic frameworks
431 MIL	Materials Institute Lavoisier
432 Na ₂ BDC	disodium terephthalate
433 NMR	nuclear magnetic resonance
434 PET	poly(ethylene terephthalate)
435 PXRD	powder X-ray diffraction
436 SEM	scanning electron microscopy
437 TGA	thermogravimetric analysis
438 TPA	terephthalic acid
439 UiO	Universitetet i Oslo
440	

441 **REFERENCES**

(1) Sillanpää, M.; Ncibi, C. *The Circular Economy: Case Studies about the Transition from the Linear Economy*; Academic Press: Cambridge, 2019.

(2) U.S. Environmental Protection Agency. Advancing Sustainable Materials Management: 2014 Fact Sheet, 2015. https://www.epa.gov/sites/default/files/2016-11/documents/2014_smmfactsheet_508.pdf.

(3) S&P Global. *Chemical Economics Handbook Polyester Fibers*; S&P Global: New York, 2022.

(4) Lalidinpuii, Z. T.; Khiangte, V.; Lalhmangaihzuala, S.; Lalmuanpuia, C.; Pachuau, Z.; Lalhriatpuia, C.; Vanlaldinpui, K. Methanolysis of PET Waste Using Heterogeneous Catalyst of Bio-Waste Origin. *J. Polym. Environ.* 2022, **30**, 1600–1614.

(5) Pingale, N. D.; Palekar, V. S.; Shukla, S. R. Glycolysis of Postconsumer Polyethylene Terephthalate Waste. *J. Appl. Polym. Sci.* 2010, **115**, 249–254.

(6) Chan, K.; Zinchenko, A. Conversion of Waste Bottles' PET to a Hydrogel Adsorbent via PET Aminolysis. *J. Environ. Chem. Eng.* 2021, **59**, No. 106129.

(7) Ügdüler, S.; Van Geem, K. M.; Denolf, R.; Roosen, M.; Mys, N.; Ragaert, K.; De Meester, S. Towards Closed-Loop Recycling of Multilayer and Coloured PET Plastic Waste by Alkaline Hydrolysis. *Green Chem.* 2020, **22**, 5376–5394.

(8) Deleu, W. P. R.; Stassen, I.; Jonckheere, D.; Ameloot, R.; De Vos, D. E. Waste PET (Bottles) as a Resource or Substrate for MOF Synthesis. *J. Mater. Chem. A* 2016, **4**, 9519–9525.

(9) Karam, L.; Miglio, A.; Specchia, S.; el Hassan, N.; Massiani, P.; Reboul, J. PET Waste as Organic Linker Source for the Sustainable Preparation of MOF-Derived Methane Dry Reforming Catalysts. *Mater. Adv.* 2021, **2**, 2750–2758.

(10) Phan, N. T. S.; Nguyen, T. T.; Nguyen, K. D.; Vo, A. X. T. An Open Metal Site Metal–Organic Framework Cu(BDC) as a Promising Heterogeneous Catalyst for the Modified Friedländer Reaction. *Appl. Catal., A* 2013, **464–465**, 128–135.

(11) Chuah, C. Y.; Li, W.; Samarsinghe, S. A. S. C.; Sethunga, G. S. M. D. P.; Bae, T. H. Enhancing the CO₂ Separation Performance of Polymer Membranes via the Incorporation of Amine-Functionalized HKUST-1 Nanocrystals. *Microporous Mesoporous Mater.* 2019, **290**, No. 109680.

(12) Du, J.; Zhang, C.; Pu, H.; Li, Y.; Jin, S.; Tan, L.; Zhou, C.; Dong, L. HKUST-1 MOFs Decorated 3D Copper Foam with Superhydrophobicity/Superoleophilicity for Durable Oil/Water Separation. *Colloids Surf., A* 2019, **573**, 222–229.

(13) Fan, W.; Wang, X.; Xu, B.; Wang, Y.; Liu, D.; Zhang, M.; Shang, Y.; Dai, F.; Zhang, L.; Sun, D. Amino-Functionalized MOFs with High Physicochemical Stability for Efficient Gas Storage/Separation, Dye Adsorption and Catalytic Performance. *J. Mater. Chem. A* 2018, **6**, 487 24486–24495.

(14) Park, Y.; Homayoonnia, S.; Kim, S.; Kim, H. W. In-Situ Fabrication of Cu-BDC on a Quartz Crystal Microbalance for Methane Sensing at Room Temperature. *J. Inclusion Phenom. Macrocyclic Chem.* 2021, **101**, 321–327.

(15) Xie, Y.; Liu, X.; Ma, X.; Duan, Y.; Yao, Y.; Cai, Q. Small Titanium-Based MOFs Prepared with the Introduction of Tetraethyl Orthosilicate and Their Potential for Use in Drug Delivery. *ACS Appl. Mater. Interfaces* 2018, **10**, 13325–13332.

(16) Ribadeneyra, M. C.; King, J.; Titirici, M. M.; Szilágyi, P. A. A Facile and Sustainable One-Pot Approach to the Aqueous and Low-Temperature PET-to-UiO-66(Zr) Upcycling. *Chem. Commun.* 2022, **58**, 1330–1333.

(17) Cosimescu, L.; Merkel, D. R.; Darsell, J.; Petrossian, G. Simple but Tricky: Investigations of Terephthalic Acid Purity Obtained from Mixed PET Waste. *Ind. Eng. Chem. Res.* 2021, **60**, 12792–12797.

(18) Doan, V. D.; Do, T. L.; Ho, T. M. T.; Le, V. T.; Nguyen, H. T. Utilization of Waste Plastic PET Bottles to Prepare Copper-1,4-Benzenedicarboxylate Metal-Organic Framework for Methylene Blue Removal. *Sep. Sci. Technol.* 2020, **55**, 444–455.

(19) Dyosiba, X.; Ren, J.; Musyoka, N. M.; Langmi, H. W.; Mathe, M.; Onyango, M. S. Preparation of Value-Added Metal-Organic Frameworks (MOFs) Using Waste PET Bottles as Source of Acid Linker. *Sustainable Mater. Technol.* 2016, **10**, 10–13.

(20) Dyosiba, X.; Ren, J.; Musyoka, N. M.; Langmi, H. W.; Mathe, M.; Onyango, M. S. Feasibility of Varied Polyethylene Terephthalate Wastes as a Linker Source in Metal-Organic Framework UiO-66(Zr) Synthesis. *Ind. Eng. Chem. Res.* 2019, **58**, 17010–17016.

(21) Lo, S. H.; Raja, D. S.; Chen, C. W.; Kang, Y. H.; Chen, J. J.; Lin, C. H. Waste Polyethylene Terephthalate (PET) Materials as Sustainable Precursors for the Synthesis of Nanoporous MOFs, MIL-47, MIL-53(Cr, Al, Ga) and MIL-101(Cr). *Dalton Trans.* 2016, **45**, 9565–9573.

(22) Li, Z.; Xia, H.; Li, S.; Pang, J.; Zhu, W.; Jiang, Y. In Situ Hybridization of Enzymes and Their Metal-Organic Framework Analogues with Enhanced Activity and Stability by Biomimetic Mineralisation. *Nanoscale* 2017, **9**, 15298–15302.

(23) Sánchez-Sánchez, M.; Getachew, N.; Díaz, K.; Díaz-García, M.; Chebude, Y.; Díaz, I. Synthesis of Metal-Organic Frameworks in Water at Room Temperature: Salts as Linker Sources. *Green Chem.* 2015, **17**, 1500–1509.

(24) Bajpe, S. R.; Breynaert, E.; Mustafa, D.; Jobbág, M.; Maes, A.; Martens, J. A.; Kirschhock, C. E. A. Effect of Keggin Polyoxometalate on Cu (II) Speciation and Its Role in the Assembly of Cu₃(BTC)₂ Metal-Organic Framework. *J. Mater. Chem.* 2011, **21**, 9768–9771.

(25) Zhang, S.; Jian, M.; Zhang, Q.; Xu, R.; Qu, J.; Luo, X.; Li, X.; Hu, J.; Liu, R.; Zhang, X. Recyclable Printed Circuit Boards and Alkali Reduction Wastewater: Approach to a Sustainable Copper-Based Metal-Organic Framework. *ACS Sustainable Chem. Eng.* 2020, **8**, 1371–1379.

(26) Rubio Arias, J. J.; Thielemans, W. Instantaneous Hydrolysis of PET Bottles: An Efficient Pathway for the Chemical Recycling of Condensation Polymers. *Green Chem.* 2021, **23**, 9945–9956.

(27) Štrukil, V. Highly Efficient Solid-State Hydrolysis of Waste Polyethylene Terephthalate by Mechanochemical Milling and Vapor-Assisted Aging. *ChemSusChem* 2021, **14**, 330–338.

(28) Noritake, A.; Hori, M.; Shigematsu, M.; Tanahashi, M. Recycling of Polyethylene Terephthalate Using High-Pressure Steam Treatment. *Polym. J.* 2008, **40**, 498–502.

(29) Ma, Y. H.; Ge, S. W.; Wang, W.; Sun, B. W. Studies on the Synthesis, Structural Characterization, Hirshfeld Analysis and Stability of Apovincamine (API) and Its Co-Crystal (Terephthalic Acid: Apovincamine = 1:2). *J. Mol. Struct.* 2015, **1097**, 87–97.

(30) Musale, R. M.; Shukla, S. R. Deep Eutectic Solvent as Effective Catalyst for Aminolysis of Polyethylene Terephthalate (PET) Waste. *Int. J. Plast. Technol.* 2016, **20**, 106–120.

553 (31) Téllez, C. A.; Hollauer, E.; Mondragon, M. A.; Castaño, V. M.
554 Fourier Transform Infrared and Raman Spectra, Vibrational Assign-
555 ment and Ab Initio Calculations of Terephthalic Acid and Related
556 Compounds. *Spectrochim. Acta, Part A* 2001, **57**, 993–1007.

557 (32) Wang, S.; Ma, J.; Zhai, X.; Zhang, X.; Fan, F.; Wang, T.; Li, Y.;
558 Zhang, L.; Fu, Y. Structural and Morphological Transformation of Two-
559 Dimensional Metal-Organic Frameworks Accompanied by Controlled
560 Preparation Using the Spray Method. *Langmuir* 2020, **36**, 7392–7399.

561 (33) Chen, J.; Si, Y.; Liu, Y.; Wang, S.; Wang, S.; Zhang, Y.; Yang, B.;
562 Zhang, Z.; Zhang, S. Starch-Regulated Copper-Terephthalic Acid as a
563 pH/Hydrogen Peroxide Simultaneous-Responsive Fluorescent Probe
564 for Lysosome Imaging. *Dalton Trans.* 2019, **48**, 13017–13025.

565 (34) Cheng, X.; Zhang, S.; Liu, H.; Chen, H.; Zhou, J.; Chen, Z.;
566 Zhou, X.; Xie, Z.; Kuang, Q.; Zheng, L. Biomimetic Metal-Organic
567 Framework Composite-Mediated Cascade Catalysis for Synergistic
568 Bacteria Killing. *ACS Appl. Mater. Interfaces* 2020, **12**, 36996–37005.

569 (35) Falcaro, P.; Okada, K.; Hara, T.; Ikigaki, K.; Tokudome, Y.;
570 Thornton, A. W.; Hill, A. J.; Williams, T.; Doonan, C.; Takahashi, M.
571 Centimetre-Scale Micropore Alignment in Oriented Polycrystalline
572 Metal-Organic Framework Films via Heteroepitaxial Growth. *Nat. Mater.* 2017, **16**, 342–348.

573 (36) Wei, X.; Chen, J.; Zhang, X.; Zhu, Z.; Liu, H.; Wang, X.; Guo, X.;
574 Yang, B. Organic Framework@Coordination Polymer Core-Shell
575 Composites as Dual-Modal Probe for Fluorescence and Colorimetric
576 Analysis of Total Antioxidant Level in Saliva. *Sens. Actuators, B* 2021,
577 **347**, No. 130588.

578 (37) Salama, R. S.; El-Hakam, S. A.; Samra, S. E.; El-Dafrawy, S. M.;
579 Ahmed, A. I. Adsorption, Equilibrium and Kinetic Studies on the
580 Removal of Methyl Orange Dye from Aqueous Solution by Using of
581 Copper Metal Organic Framework (Cu-BDC). *Int. J. Mod. Chem.* 2018,
582 **10**, 195–207.

583 (38) Nanthamathee, C. Effect of Co (II) Dopant on the Removal of
584 Methylene Blue by a Dense Copper Terephthalate. *J. Environ. Sci.* 2019,
585 **81**, 68–79.

586 (39) Wang, S.; Yu, Y.; Yu, J.; Wang, T.; Wang, P.; Li, Y.; Zhang, X.;
587 Zhang, L.; Hu, Z.; Chen, J.; Fu, Y.; Qi, W. Encapsulation of Metal Oxide
588 Nanoparticles inside Metal-Organic Frameworks via Surfactant-
589 Assisted Nanoconfined Space. *Nanotechnology* 2020, **31**, No. 255604.

590 (40) Low, J. J.; Benin, A. I.; Jakubczak, P.; Abrahamian, J. F.; Faheem,
591 S. A.; Willis, R. R. Virtual High Throughput Screening Confirmed
592 Experimentally: Porous Coordination Polymer Hydration. *J. Am. Chem.
593 Soc.* 2009, **131**, 15834–15842.

594 (41) Alvarez, J. R.; Sánchez-González, E.; Pérez, E.; Schneider-
595 Revueltas, E.; Martínez, A.; Tejeda-Cruz, A.; Islas-Jácome, A.;
596 González-Zamora, E.; Ibarra, I. A. Structure Stability of HKUST-1
597 Towards Water and Ethanol and Their Effect on Its CO₂ Capture
598 Properties. *Dalton Trans.* 2017, **46**, 9192–9200.

599 (42) Ryu, U. J.; Jee, S.; Rao, P. C.; Shin, J.; Ko, C.; Yoon, M.; Park, K.;
600 Choi, K. M. Recent Advances in Process Engineering and Upcoming
601 Applications of Metal-Organic Frameworks. *Coord. Chem. Rev.* 2021,
602 **426**, No. 213544.

603 (43) Jiamjirangkul, P.; Inprasit, T.; Intasanta, V.; Pangon, A. Metal
604 Organic Framework-Integrated Chitosan/Poly(vinyl alcohol) (PVA)
605 Nanofibrous Membrane Hybrids from Green Process for Selective CO₂
606 Capture and Filtration. *Chem. Eng. Sci.* 2020, **221**, No. 115650.

607 (44) Muttakin, M.; Mitra, S.; Thu, K.; Ito, K.; Saha, B. B. Theoretical
608 Framework to Evaluate Minimum Desorption Temperature for IUPAC
609 Classified Adsorption Isotherms. *Int. J. Heat Mass Transfer* 2018, **122**,
610 795–805.

611